ChemPubSoc Europe

DOI: 10.1002/cphc.201900364

CHEMPHYSCHEM Articles

Quantitative Assessment of B–B–B, B–H_b–B, and B–H_t Bonds: From BH_3 to $B_{12}H_{12}^{2-}$

Daniel Sethio,[a] Latévi Max Lawson Daku,[b] Hans Hagemann,[b] and Elfi Kraka*[a]

We report the thermodynamic stabilities and the intrinsic strengths of three-center-two-electron B–B–B and B–H_b–B bonds (H_b: bridging hydrogen), and two-center-two-electron B–H_t bonds (H_t: terminal hydrogen) which can be served as a new, effective tool to determine the decisive role of the intermediates of hydrogenation/dehydrogenation reactions of borohydride. The calculated heats of formation were obtained with the G4 composite method and the intrinsic strengths of B–B–B, B–H_b–B, and B–H_t bonds were derived from local stretching force constants obtained at the B3LYP-D2/cc-pVTZ level of theory for 21 boron-hydrogen compounds, including 19 intermediates. The Quantum Theory of Atoms in Molecules (QTAIM) was used to deepen the inside into the nature of B–B–B, B–H_b–B, and B–H_t bonds. We found that all of the experimentally identified intermediates hindering the reversibility of the decomposition reactions are thermodynamically stable and possess strong B–B–B, B–H_b–B, and B–H_t bonds. This proves that thermodynamic data and intrinsic B–B–B, B–H_b–B, and B–H_t bond strengths form a new, effective tool to characterize new (potential) intermediates and to predict their role for the reversibility of the hydrogenation/dehydrogenation reactions.

1. Introduction

Boron-hydrogen compounds are receiving a lot of attention due to their diverse physical and chemical properties,[1–6] which can be useful for various technological applications ranging from hydrogen storage,[7] fuel cells[8] to high conducting materials even at room temperature[9–11] as well as for applications in medicinal chemistry.[12–15] Boranes and carboranes are recently targeted because of their potential to form BH $\cdots$ π interactions with the π-face of an arene.[16–19] It has been suggested that these BH $\cdots$ π interactions may be driven by a nonspecific weak dispersion contact, as for example based on restrained fit to the electrostatic potential and symmetry-adapted perturbation theory studies[20,21] or molecular orbital analyses.[22] However, these approaches are not free from some arbitrariness, therefore they are generally not suited for deriving more definite conclusions on a particular bonding situation.[16] In a combined experimental and theoretical study on several iridium-dimercapto-carborane complexes Zhang, Zou and co-workers verified the existence of this new nonclassical BH $\cdots$ π H-bond in both, solid state and solution at ambient temperatures.[16,17] They could also show that the bond strength of the BH $\cdots$ π H-bond as determined via the Konkoli-Cremer local mode analysis[23–26] is comparable to what is found for the H-bond in the water dimer.[27,28] The same holds for the binding energy, which is in both cases in the range of 5 kcal/mol. However, in contrast to the water-dimer the BH $\cdots$ π H-bond is electrostatic in nature as confirmed by the topological analysis of the electron density $\rho(\mathbf{r})$.[28]

Closo-boranes have shown remarkably high ionic conductivities and stabilities at or near room temperature, making them suitable for the use in rechargeable battery applications.[9,10,29–31] Recently, a stable 3 V battery prototype has been successfully assembled using, for example, the $Na_2(B_{12}H_{12})_{0.5}(B_{10}H_{10})_{0.5}$ electrolyte.[9,32] On the other, metal borohydrides have attracted considerable interest due to their potential as hydrogen storage materials.[5,6,33,34] These compounds have a high gravimetric hydrogen content[35,36] which can be used for mobile applications.[36–40]

The actual use of boron-hydrogen compounds as hydrogen storage materials has been constrained by their thermodynamics and kinetics properties, and the reversibility of their intermediates.[41–43] Many hydrogenation and dehydrogenation reactions take place at extreme reaction conditions (such as high pressure and high temperature) and are kinetically too slow for practical use.[44–46] The formation of intermediate species may hinder the reversibility of the reactions.

Thermal decomposition pathways of borohydrides (BH_4^- (**2**)) are of multi-step character and complex (see Figure 1 and Figure 2).[43] Some intermediates, such as B_2H_6 (**3**), $B_{10}H_{10}^{2-}$ (**18**), and $B_{12}H_{12}^{2-}$ (**21**)[47–50] have been observed during the decomposition of $LiBH_4$. The formation of $LiB_{12}H_{12}$ has been confirmed by NMR[51] and Raman spectroscopy.[52] The formation of $B_{12}H_{12}^{2-}$ (**21**) hampers the reversibility of the reactions due to its thermodynamic stability.[37,53–57] Other intermediates, such as $B_2H_7^-$ (**4**), $B_3H_8^-$ (**5**), $B_{10}H_{10}^{2-}$ (**18**), and $B_{12}H_{12}^{2-}$ (**21**), have been reported during the decomposition of $Mg(BH_4)_2$.[6,58–60] On the other hand, the formation of $B_3H_8^-$ (**3**) facilitates the reversibility of the reaction.[6,61,62] Thermal decomposition of borohydrides and its reverse reactions involve the breaking and forming of B–B–B, B–H_b–B, and B–H_t bonds. The structural[63–65] and spectroscopic properties,[66–70] as well as nature of bridging

[a] Dr. D. Sethio, Prof. E. Kraka
Computational and Theoretical Chemistry Group (CATCO), Department of Chemistry, Southern Methodist University, 3215 Daniel Avenue, Dallas, Texas 75275-0314, United States
E-mail: ekraka@gmail.com
[b] Dr. L. M. L. Daku, Prof. H. Hagemann
Department of Physical Chemistry, University of Geneva, 30 Quai Ernest-Ansermet, CH-1211 Geneva 4, Switzerland

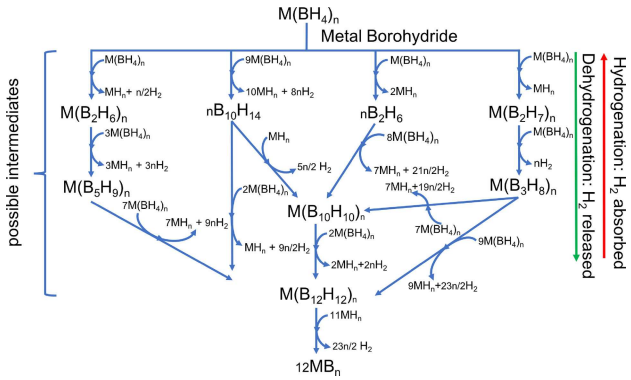

Figure 1. Schematic (selected) decomposition pathways from metal borohydride **2** to MB_n through intermediates B_2H_6 (**3**), $B_2H_7^-$ (**4**), $B_3H_8^-$ (**5**), $B_{10}H_{10}^{2-}$ (**18**), $B_{10}H_{14}$ (**19**), and $B_{12}H_{12}^{2-}$ (**21**).

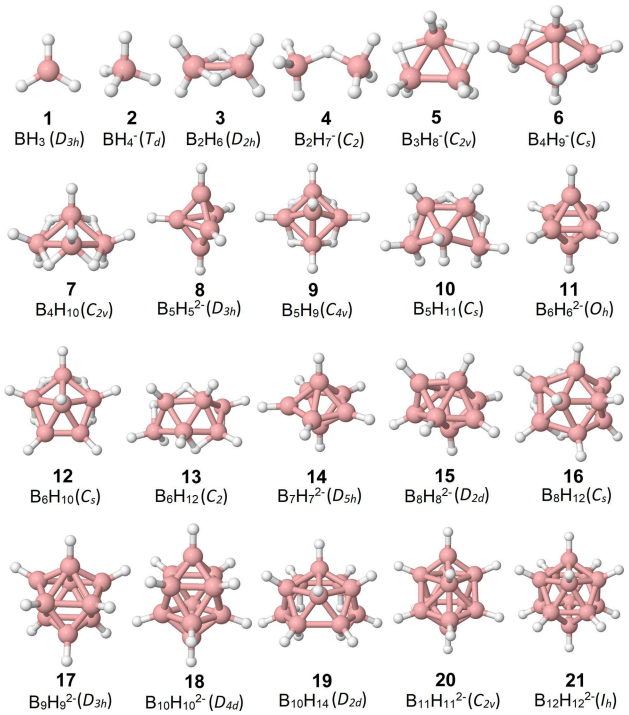

Figure 2. Structures of 21 boron-hydrogen compounds: BH_3 (**1**), BH_4^- (**2**), B_2H_6 (**3**), $B_2H_7^-$ (**4**), $B_3H_8^-$ (**5**), $B_4H_9^-$ (**6**), B_4H_{10} (**7**), $B_5H_5^{2-}$ (**8**), B_5H_9 (**9**), B_5H_{11} (**10**), $B_6H_6^{2-}$ (**11**), B_6H_{10} (**12**), B_6H_{12} (**13**), $B_7H_7^{2-}$ (**14**), $B_8H_8^{2-}$ (**15**), B_8H_{12} (**16**), $B_9H_9^{2-}$ (**17**), $B_{10}H_{10}^{2-}$ (**18**), $B_{10}H_{14}$ (**19**), $B_{11}H_{11}^{2-}$ (**20**), and $B_{12}H_{12}^{2-}$ (**21**). Intermediate species are from B_2H_6 (**3**) to $B_{12}H_{12}^{2-}$) (**21**), where B_2H_6 (**3**), $B_2H_7^-$ (**4**), $B_3H_8^-$ (**5**), $B_{10}H_{10}^{2-}$ (**18**), $B_{10}H_{14}$ (**19**), and $B_{12}H_{12}^{2-}$ (**21**) have been observed during the decomposition of metal borohydride.

hydrogen and BB bonds[71,72] have been studied by different authors. However, to the best of our knowledge, a systematic and detailed study of the intrinsic strengths of the B–B, B–H_b, and B–H_t bonds of the intermediate compounds and their role for the reversibility of hydrogenation/dehydrogenation reactions are still missing.

Vibrational spectroscopy is a useful tool to identify and characterize molecules, which so far has not been explored to its full extent. Konkoli and Cremer have refined the use of vibrational spectroscopy to define intrinsic bond strengths via local vibrational modes.[23,24] The associated local stretching force constants k^a are used to probe the intrinsic strength of chemical bonds.[25,73–75] It has been shown that the local stretching force constant k^a is a superior bond strength measure compared to the often used bond dissociation energies (BDE) and bond dissociation enthalpies (BDH) as they contain cumulative effects of geometry relaxation, multiple bonding interactions, and also electronic density reorganizations of the dissociated fragments.[73,76,77] Local stretching force constants k^a have been successfully used to determine the intrinsic bond strength of covalent bonds such as: CC bonds,[74,75,78,79] NN bonds,[80] NF bonds,[81] CO bonds,[82] and CX (X = F, Cl, Br, I) bonds,[83–86] and weak chemical interactions such as: hydrogen bonding,[87–90] halogen bonding,[91–93] pnicogen bonding,[94–96] chalcogen bonding,[73,77] tetrel bonding,[97] and recently BH $\cdots$ π interactions.[16,17]

The main objectives of this paper are: (i) to evaluate the nature of the B–B, B–H_b, and B–H_t bonds; (ii) to evaluate why intermediate species may or may not facilitate the reversibility reactions in the perspective of thermodynamics and intrinsic bond strength; (iii) to provide a new tool to characterize new (potential) intermediates and their role for the reversibility of the hydrogenation/dehydrogenation reactions; and (iv) to give guidelines whether intermediates may be stable enough to be isolated. To fulfill the objectives, we accurately determined the heats of formation and the local stretching force constants k^a of 21 boron-hydrogen compounds including 19 intermediates (see Figure 2): closoboranes ($B_xH_x^{2-}$), nidoboranes (B_xH_{x+4} and $B_xH_{x+3}^-$), and arachnoboranes (B_xH_{x+6} and $B_xH_{x+5}^-$). Quantum theory of atoms in molecules (QTAIM) analyses was performed in addition, to understand the nature of these bonds.

Computational Methods

Equilibrium geometries and normal vibrational modes of 21 boron hydrogen compounds (see Figure 2) were obtained using the procedure reported in Ref. [98–101] for an accurate prediction of boron hydrogen compounds. Thus, the B3LYP functional[102] augmented with Grimme's semi-empirical D2[103] dispersion correction was used in combination with the Dunning correlation-consistent cc-pVTZ basis set.[104,105] The inclusion of dispersion correction improves the structural parameters of the bridging hydrogen.[99,101] The vibrational analysis performed on each equilibrium geometry showed that it corresponds to a minimum on the potential energy surface (no imaginary vibrational frequencies).

The heats of formation were calculated using the G4 model chemistry.[106] The G4 protocol isa composite method, where the equilibrium geometries and frequencies calculation are calculated at B3LYP/6-31G(2df,p) level of theory, whereas the energies are corrected to the Hartree-Fock energy limit, and single point calculations obtained at the Coupled Cluster theory with singles, doubles, and perturbative triples (CCSD(T)) and the complete fourth-order Møller-Plesset perturbation theory (MP4).[106] The G4 theory provides very accurate predictions of thermodynamics data with an average deviation 0.83 kcal/mol from experimental data for a test set of 454 molecules.[106]

Nguyen and co-workers used isodesmic and similar types of reactions to determine the heats of formation of several boron-

hydrogen compounds from calculated reaction energies and known heats of formation of reactants and products.[107,108] Going along the same line, we used the hydrogenation reactions given by Eq 1–Eq 4, where known heats of formation were used to calculate unknown heats of formation.

$$B_xH_{x+4} + (x-2)H_2 \rightarrow xBH_3 \quad (1)$$

$$B_2H_7^- \rightarrow BH_3 + BH_4^- - \quad (2)$$

$$B_3H_8^- + H_2 \rightarrow BH_4^- + 2BH_3 \quad (3)$$

$$B_xH_x^{2-} + (x-1)H_2 \rightarrow 2BH_4^- + (x-2)BH_3 \quad (4)$$

where x = 2,…,12.

The heats of formation of H_2, BH_3 (**1**), and BH_4^- (**2**) were determined using the total atomization energies given by Eq 5–Eq 7. The heats of formation of B and H atoms were obtained from the thermodynamic database (NIST-JANAF Tables).[109]

$$H_2 \rightarrow 2H \quad (5)$$

$$BH_3 \rightarrow B + 3H \quad (6)$$

$$BH_4^- \rightarrow B + 4H + e \quad (7)$$

Vibrational spectroscopy provides important information about the electronic structure of a molecule and can be used to access the intrinsic strength of a bond. However, normal vibrational modes are of limited use due to mode-mode coupling, *e.g.* electronic and kinematic (mass) coupling.[23] The electronic coupling is eliminated by solving the Wilson equation.[110] The resulting normal modes are delocalized in the molecular framework as a consequence of kinematic (mass) coupling. Konkoli and Cremer showed that solving a mass-decoupled equivalent of the Wilson equation leads to local vibrational modes, which are associated with a given internal coordinate, q_n, (bond length, bond angle, and dihedral angle, etc.).[23,24] Zou and Cremer proved that there is a one-to-one relationship between the local and the normal vibrational modes, which can be verified with the Adiabatic Connection Scheme (ACS).[25]

For simplification, the local force constants, k^a, of B–B–B, B–H_b–B and B–H_t bonds can be converted into bond strength orders, BSO $n(BBB)$, BSO $n(BHB)$ and BSO $n(BH)$, using a power relationship:[23,26]

$$BSO_n = a(k^a)^b \quad (8)$$

The constants a and b can be obtained from the k^a values of two reference molecules which have well-defined bond order. In the present work, the BSO values BSO $n(BH)$ were derived by using the BH bonds in BH_3 and $B_2H_7^-$ as reference, which have the k^a values of 3.863 and 1.632 mdyn/Å, respectively and correspond to Wiberg bond indices[111,112] of $n(BH) = 0.984$ in BH_3 and $n(BH) = 0.498$ in $B_2H_7^-$. The BSO values $n(BBB)$ were determined from the BB bonds in B_2H_6 and $B_2H_7^-$ which have k^a values of 2.391 and 0.296 mdyn/Å, respectively and correspond to Wiberg bond indices of $n(BB) = 0.662$ in B_2H_6 and $n(BB) = 0.265$ in $B_2H_7^-$. It also assumed that $k^a = 0$ refers to BSO $n = 0$. The values of k^a and BSO n were taken as averages over all B–B–B, B–H_b–B, and B–H_t bonds.

All calculations were performed using the Gaussian09 package.[113] The geometries were optimized with ultrafine grid integration[114] and tight convergence criteria for the forces and displacements. Local mode force constants and frequencies[23] were calculated using COLOGNE2017.[115]

The electron density (ρ_c) and the total energy density (H_c) at the B–B–B and B – H_b – H ring critical points, and at B–H_t bond critical points[116–118] were calculated using the AIMAll program.[119] The Cremer-Kraka criteria were used to identify the covalent character of the bonds.[120–122] A negative value of the total energy density ($itH_c < 0$) at bond critical point (BCP) on the bond path between two atoms A and B forming C bond indicates a covalent interaction, while a positive value ($H_c > 0$) points to electrostatic interaction.

2. Results and Discussion

In this Section, first, the structures of 21 boron-hydrogen compounds are discussed, showing that the chosen B3LYP-D2 model chemistry provides reasonable geometries compared to experimental data. Second, the heats of formation of the studied compounds are discussed, followed by the intrinsic strength of the 3c–2e B–B–B and B–H_b–B bonds (H_b: bridging hydrogen), and 2c–2e B – H_t bonds (H_t: terminal hydrogen). Third, thermal decomposition of borohydride, intermediates, and their reversibility are discussed, showing that the combination of thermodynamic data and intrinsic bond strengths forms a new powerful tool to characterize the nature of the B–B–B, B – H_b – H, and B–H_t of the intermediates and to disclose their role for the reversibility of hydrogenation/dehydrogenation reactions. Last, the use of local mode analysis as a predictive tool to guide whether intermediates may be stable enough to be isolated are discussed.

The studied 21 boron-hydrogen compounds include closoboranes ($B_xH_x^{2-}$: $B_5H_5^{2-}$ (**8**), $B_6H_6^{2-}$ (**11**), $B_7H_7^{2-}$ (**14**), $B_8H_8^{2-}$ (**15**), $B_9H_9^{2-}$ (**17**), $B_{10}H_{10}^{2-}$ (**18**), $B_{11}H_{11}^{2-}$ (**20**), $B_{12}H_{12}^{2-}$ (**21**)), nidoboranes (B_xH_{x+4} and $B_xH_{x+3}^-$: BH_4^- (**2**), B_2H_6 (**3**), B_5H_9 (**9**), B_6H_{10} (**12**), B_8H_{12} (**16**), $B_{10}H_{14}$ (**19**)), arachnoboranes (B_xH_{x+6} and $B_xH_{x+5}^-$: $B_2H_7^-$ (**4**), $B_3H_8^-$ (**5**), $B_4H_9^-$ (**6**), B_4H_{10} (**7**), B_5H_{11} (**10**), B_6H_{12} (**13**)), and BH_3 (**1**).

2.1. Structure of 21 Boron-Hydrogen Compounds

Table 1 and Figure 2 summarize the experimental and calculated average bond lengths of the 21 boron-hydrogen compounds studied in this work. The calculated bond lengths obtained at B3LYP-D2/cc-pVTZ level of theory are in good agreement with experimental data. For example, the calculated B–H_t in BH_3 (**1**) (Calc. 1.189 Å) shows an excellent agreement with the experimental data obtained by gas-phase high-resolution infra-red spectroscopy (Exp. 1.185 Å).[123] The largest deviation is about 0.08 Å for B–H_b in $B_3H_8^-$ (**5**), where the experimental values were recorded using X-ray spectroscopy on solid NaB_3H_8.[127] A larger deviation from experimental data was expected (as we do not take into account the counter ions and the influence of their environment in crystals).

Table 1. Average lengths of the B–B, B–H_b, and B–H_t bonds (in Å) of $B_xH_y^{z-}$ species (x = 1-12, y = 3-14, z = 0-2)) calculated at the B3LYP-D2/cc-pVTZ level of theory.

#	Molecule, Symm.	Fragment	Calc.	Exp.	Fragment	Calc.	Exp.
1	BH_3, D_{3h}	B–H_t	1.189	1.185[a]			
2	BH_4^-, T_d	B–H_t	1.237	1.215[b]			
3	B_2H_6, D_{2h}	B–H_t	1.186	1.182(11)[c]	B–B	1.761	1.747(7)[c]
		B–H_b	1.315	1.303(11)[c]			
4	$B_2H_7^-$, C_2	B–H_t	1.212		B–B	2.383	
		B–H_b	1.315	1.32[d]			
5	$B_3H_8^-$, C_{2v}	B–H_t	1.207	1.13(2)[e]	B–B	1.826	1.820(5)[e]
		B–H_b	1.261	1.345(2)[e]			
6	$B_4H_9^-$, C_s	B–H_t	1.201		B–B	1.784	
		B–H_b	1.339				
7	B_4H_{10}, C_{2v}	B–H_t	1.186		B–B	1.724	1.704[f]
		B–H_b	1.335	1.315[f]			
8	$B_5H_5^{2-}$, D_{3h}	B–H_t	1.211		B–B	1.672	
9	B_5H_9, C_{4v}	B–H_t	1.178		B–B	1.691	1.690[g]
		B–H_b	1.346	1.352[g]			
10	B_5H_{11}, C_s	B–H_t	1.190		B–B	1.739	1.741[h]
		B–H_b	1.334				
11	$B_6H_6^{2-}$, O_h	B–H_t	1.209	1.14(2)[i]	B–B	1.730	1.726(2)[i]
12	B_6H_{10}, C_s	B–H_t	1.180		B–B	1.695	1.654[g]
		B–H_b	1.333				
13	B_6H_{12}, C_2	B–H_t	1.184		B–B	1.722	1.778[h]
		B–H_b	1.325	1.308[h]			
14	$B_7H_7^{2-}$, D_{5h}	B–H_t	1.210		B–B	1.767	1.735[j]
15	$B_8H_8^{2-}$, D_{2d}	B–H_t	1.208		B–B	1.794	1.74(2)[k]
16	B_8H_{12}, C_s	B–H_t	1.179	1.115[l]	B–B	1.784	1.789[j]
		B–H_b	1.339				
17	$B_9H_9^{2-}$, D_{3h}	B–H_t	1.203		B–B	1.711	1.71[m]
18	$B_{10}H_{10}^{2-}$, D_{4d}	B–H_t	1.200	1.181[n]	B–B	1.702	1.727[n]
19	$B_{10}H_{14}$, D_{2d}	B–H_t	1.180	1.173[o]	B–B	1.783	1.785[o]
		B–H_b	1.324				
20	$B_{11}H_{11}^{2-}$, C_{2v}	B–H_t	1.200		B–B	1.744	1.746[p]
21	$B_{12}H_{12}^{2-}$, I_h	B–H_t	1.198	1.20[q]	B-B	1.788	1.78[q]

Experimental values were taken from [a]Ref. [123], [b]Ref. [124], [c]Ref. [125], [d]Ref. [126], [e]Ref. [127], [f]Ref. [128], [g]Ref. [129], [h]Ref. [130], [i]Ref. [131], [j]Ref. [132], [k]Ref. [133], [l]Ref. [134], [m]Ref. [135], [n]Ref. [136], [o]Ref. [137], [p]Ref. [138], [q]Ref. [139]

2.2. Heats (Enthalpies) of Formation

Table 2 compares the experimental and calculated heats of formation obtained from B3LYP-D2, G3, G3B3, G4, and CCSD(T)/CBS methods. B3LYP-D2 results have the largest deviation from the experimental values with a RMSD of 13.32 kcal/mol. G3 and G3B3 give comparable results with RMSD values of 10.01 and 9.38 kcal/mol, respectively. CCSD(T) performs better than the aforementioned methods with a RMSD of 6.6 kcal/mol.

G4 is superior to the other methods with RMSD of 3.61 kcal/mol. Curtiss noted that the inclusion of energy corrections at the Hartree-Fock limit, CCSD(T), and the MP4 contributes to the significant improvement of the G4 method.[106] The calculated heats of formation obtained from the G4 deviate 0.08 to 9.37 kcal/mol from the experimental values, where the significant deviations are observed for *n* larger than 6 (*n* is the number of boron atoms). It is noteworthy that the experimental heats of formation of $B_{10}H_{14}$ (**19**) range from 4.4 to 11.2 kcal/mol (see Table 2).[140] Moreover, Nguyen and co-workers argued that the values of a T1 diagnostic (from the CCSD(T)) are small, indicating that boron-hydrogen compounds do not possess significant multireference character; thus, suggesting the heats of formation of boron-hydrogen compounds need to be remeasured.[107]

Inspection of Table 2 and Figure 3 shows that the highest heat of formation (positive ΔH_f^o, the amount of energy or heat absorbed during the formation of the substance) is that for $B_5H_5^{2-}$ (**8**) and the lowest (negative ΔH_f^o, the amount of energy or heat released during the formation of the substance) is that for $B_{12}H_{12}^{2-}$ (**21**). The heats of formation values of closoboranes, from penta-closoborane ($B_5H_5^{2-}$ (**8**)) to dodeca-closoborane ($B_{12}H_{12}^{2-}$ (**21**)) show a gradual decrease from +109.91 to −102.43 kcal/mol. It is also noteworthy that

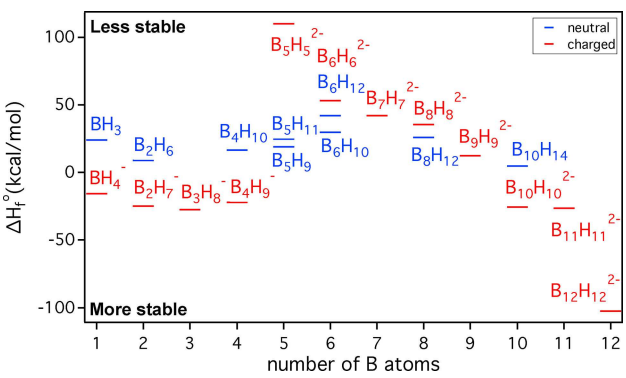

Figure 3. Heats of formation of 21 boron-hydrogen compounds calculated at the G4 level of theory as a function of number of boron atoms.

Table 2. Experimental and calculated heats of formation at STP (ΔH_f°) of the $B_xH_y^{z-}$ species (x = 1-12, y = 3-14, z = 0-2) calculated using DFT (B3LYP-D2/cc-pVTZ), G3[a], G3B3[a], CCSD(T)/CBS[a], and G4 level of theory (in kcal/mol)*.

#	Molecule, Symm.	DFT	G3[a]	G3B3[a]	CCSD(T)/CBS[a]	G4	Exp.
1	BH_3, D_{3h}	19.53	25.4	25.7	–	23.97	21.3[b]
2	BH_4^-, T_d	−20.27	−13.9	−13.5	–	−15.52	
3	B_2H_6, D_{2h}	1.21	–	–	–	8.78	8.7[b]
4	$B_2H_7^-$, C_2	−35.07	–	–	–	−24.85	
5	$B_3H_8^-$, C_{2v}	−37.19	−23.1	−22.6	-23.1	−27.42	
6	$B_4H_9^-$, C_s	−33.55	–	–	–	−22.29	
7	B_4H_{10}, C_{2v}	2.95	–	-	–	16.50	15.8[b]
8	$B_5H_5^{2-}$, D_{3h}	114.11	117.5	116.7	119.4	109.91	
9	B_5H_9, C_{4v}	9.09	26.4	26.2	24.1	18.83	17.5 ± 1.6 [b]
10	B_5H_{11}, C_s	9.81	–	–	–	24.78	24.7[b]
11	$B_6H_6^{2-}$, O_h	59.97	62.7	61.4	64.1	53.12	
12	B_6H_{10}, C_s	13.66	–	–	–	25.56	22.6[b]
13	B_6H_{12}, C_2	12.68	–	–	–	29.85	26.5[c]
14	$B_7H_7^{2-}$, D_{5h}	46.93	51.8	50.6	–	41.91	
15	$B_8H_8^{2-}$, D_{2d}	39.55	46.1	44.9	–	35.26	
16	B_8H_{12}, C_s	11.10	–	–	–	25.83	35.2[b]
17	$B_9H_9^{2-}$, D_{3h}	16.16	24.4	23.0	–	12.21	
18	$B_{10}H_{10}^{2-}$, D_{4d}	−21.00	−12.5	−13.9	–	−25.72	
19	$B_{10}H_{14}$, D_{2d}	−10.67	18.7	17.4	–	4.78	11.2[b], 4.4[c]
20	$B_{11}H_{11}^{2-}$, C_{2v}	−23.65	−11.8	−13.5	–	−26.33	
21	$B_{12}H_{12}^{2-}$, I_h	−99.53	−86.3	−88.1	–	−102.43	
	RMSD	13.32	10.01	9.38	6.6	3.61	

*This work: B3LYP-D2/cc-pVTZ and G4 level of theory, [a]CBS: Complete basis set limit. The values were taken from Ref. [107], [b]The experimental values were taken from Ref. [109], [c]The experimental values were taken from Ref. [140].

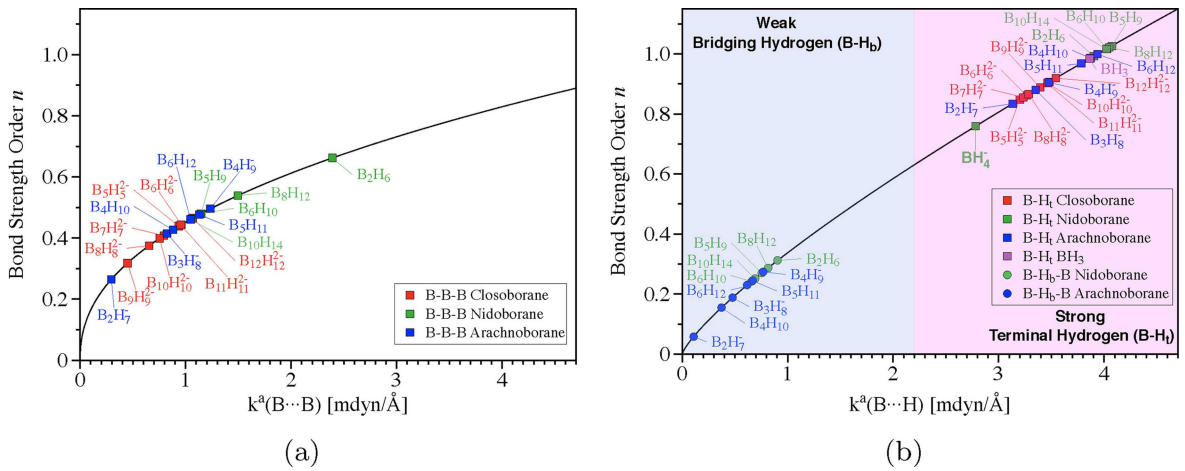

Figure 4. (a) B–B–B and (b) B–H_b–B and B–H_t bond strength order (BSO *n*) of 21 boron-hydrogen compounds calculated at B3LYP-D2/cc-pVTZ level of theory.

the larger the number of B atoms contained in a boron-hydrogen compound, that compound tends to be more stable as more energy is stored in the chemical bonds (see Table 2 and Figure 3).

2.3. The Strength of B–B–B, B–H_b–B, and B–H_t Bonds

Table 3 summarizes the bond distances, the corresponding local mode force constants, the bond strength orders, the local mode frequencies, the electron densities ρ_c, the energy densities H_c, and the energy density ratios (H_c/ρ_c) for all B–B–B, B–H_b–B, and B–H_t bonds taken as averages over all B–B–B, B–H_b–B, and B–H_t bonds. Based on the Cremer-Kraka criteria,[120–122] the B–B–B, B–H_b–B, and B–H_t bonds in the 21 boron-hydrogen compounds are covalent, and involves multicenter bonds. Due to their multi-center character, the bond strength order of the B–B–B and B–H_b–B bonds are fractional and have BSO values less than 1.

Figure 4 shows the exponential relationship between the relative bond strength order (BSO) and the local stretching force constants of B–B–B, B–H_b–B, and B–H_t bonds of the 21 boron-hydrogen compounds. The bond strength orders of the multicenter B–B–B bonds of the 21 boron-hydrogen compounds range from 0.265 to 0.662 (local mode force constant (k^a): 0.296 to 2.391 mdyn/Å), which are weaker than the single C–C bond in C_2H_6 (k^a: 4.216 mdyn/Å).[74,75,78,79] The weakest and

Table 3. Bond distances r(Å), local mode force constant k^a(mdyn/Å), bond strength order n, local mode frequencies ω^a(cm^{-1}), electron densities ρ_c(e/Å^3), energy densities H_c(h/Å^3), and the energy density ratios H_c/ρ_c of B–B–B, B–H_b–B, and B–H_t bonds.

#	Molecule, Symm.	Fragment	r	k^a	n	$\omega^{tit\ a}$	ρ_c	H_c	H_c/ρ_c
1	BH_3, D_{3h}	B–H_t	1.189	3.863	0.984	2665	1.281	−1.436	−1.121
2	BH_4^-, T_d	B–H_t	1.237	2.781	0.759	2261	1.014	−1.002	−0.988
3	B_2H_6, D_{2h}	B–H_t	1.186	3.903	0.992	2678	1.271	−1.411	−1.110
		B–B		2.391	0.662	859	0.794	−0.460	−0.580
		B–H_b–B		0.904	0.312	1734	0.794	−0.460	−0.580
4	$B_2H_7^-$, C_2	B–H_t	1.212	3.134	0.834	2399	1.127	−1.179	−1.046
		B–B		0.296	0.265	302	0.651	−0.284	−0.436
		B–H_b–B		0.109	0.058	607	0.651	−0.284	−0.436
5	$B_3H_8^-$, C_{2v}	B–H_t	1.207	3.351	0.880	2482	1.141	−1.197	−1.049
		B–B–B		0.824	0.415	614	0.760	−0.333	−0.438
		B–H_b–B		0.477	0.188	1233	0.760	−0.445	−0.585
6	$B_4H_9^-$, C_s	B–H_t	1.201	3.474	0.905	2527	1.159	−1.225	−1.057
		B–B–B		1.234	0.496	740	0.806	−0.444	−0.550
		B–H_b–B		0.768	0.274	1560	0.781	−0.541	−0.693
7	B_4H_{10}, C_{2v}	B–H_t	1.186	3.871	0.986	2667	1.261	−1.391	−1.103
		B–B–B		0.880	0.427	623	0.714	−0.325	−0.455
		B–H_b–B		0.373	0.155	1155	0.654	−0.343	−0.524
8	$B_5H_5^{2-}$, D_{3h}	B–H_t	1.211	3.201	0.848	2425	1.060	−1.066	−1.005
		B–B–B		0.935	0.439	677	0.705	−0.357	−0.506
9	B_5H_9, C_{4v}	B–H_t	1.178	4.074	1.026	2737	1.267	−1.401	−1.105
		B–B–B		1.147	0.480	743	0.680	−0.269	−0.396
		B–H_b–B		0.755	0.270	1577	0.592	−0.227	−0.383
10	B_5H_{11}, C_s	B–H_t	1.190	3.783	0.968	2634	1.234	−1.348	−1.089
		B–B–B		1.130	0.477	719	0.702	−0.318	−0.453
		B–H_b–B		0.668	0.245	1502	0.616	−0.237	−0.385
11	$B_6H_6^{2-}$, O_h	B–H_t	1.209	3.266	0.862	2450	1.081	−1.100	−1.018
		B–B–B		0.960	0.444	665	0.800	−0.376	−0.470
12	B_6H_{10}, C_s	B–H_t	1.180	4.027	1.017	2721	1.272	−1.408	−1.108
		B–B–B		1.145	0.480	734	0.632	−0.282	−0.446
		B–H_b–B		0.658	0.242	1487	0.537	−0.165	−0.306
13	B_6H_{12}, C_2	B–H_t	1.184	3.937	0.999	2690	1.268	−1.404	−1.107
		B–B–B		1.046	0.461	702	0.599	−0.204	−0.340
		B–H_b–B		0.616	0.230	1453	0.557	−0.210	−0.377
14	$B_7H_7^{2-}$, D_{5h}	B–H_t	1.210	3.234	0.855	2438	1.087	−1.110	−1.020
		B–B–B		0.793	0.408	617	0.727	−0.330	−0.454
15	$B_8H_8^{2-}$, D_{2d}	B–H_t	1.208	3.285	0.866	2457	1.102	−1.133	−1.028
		B–B–B		0.654	0.375	563	0.763	−0.363	−0.476
16	B_8H_{12}, C_s	B–H_t	1.179	4.048	1.022	2728	1.274	−1.412	−1.108
		B–B–B		1.495	0.539	822	0.923	−0.567	−0.614
		B–H_b–B		0.815	0.287	1602	0.843	−0.524	−0.621
17	$B_9H_9^{2-}$, D_{3h}	B–H_t	1.203	3.394	0.888	2498	1.119	−1.158	−1.035
		B–B–B		0.448	0.318	560	0.800	−0.467	−0.584
18	$B_{10}H_{10}^{2-}$, D_{4d}	B–H_t	1.200	3.464	0.903	2524	1.131	−1.177	−1.041
		B–B–B		0.754	0.399	590	0.678	−0.263	−0.388
19	$B_{10}H_{14}$, D_{2d}	B–H_t	1.180	4.022	1.016	2719	1.277	−1.417	−1.110
		B–B–B		1.058	0.463	699	0.753	−0.324	−0.430
		B–H_b–B		0.692	0.252	1527	0.258	−0.017	−0.066
20	$B_{11}H_{11}^{2-}$, C_{2v}	B–H_t	1.200	3.482	0.907	2530	1.141	−1.193	−1.045
		B–B–B		0.954	0.443	662	0.718	−0.299	−0.416
21	$B_{12}H_{12}^{2-}$, I_h	B–H_t	1.198	3.541	0.919	2551	1.153	−1.212	−1.051
		B–B–B		1.067	0.465	702	0.747	−0.316	−0.423

*The values were taken as averages over all B–B–B, B–H_b–B, and B–H_t bonds.The electron densities ρ_c and energy densities H_c of B–B bonds of B_2H_6 (**3**) and $B_2H_7^-$ (**4**) are obtained from the middle point between two boron atoms.

the strongest B–B–B bonds are found in $B_2H_7^-$ (**4**) and B_2H_6 (**12**), respectively.

The B–H_t bonds are weaker than the C–H bonds in CH_4 (k^a: 5.367 mdyn/Å.[74,75,78,79] The B–H_b–B bonds (BSO: 0.058–0.312, k^a: 0.109–0.904 mdyn/Å) are significantly weaker and longer than the B–H_t bonds (BSO: 0.759–1.026, k^a: 2.781–4.074 mdyn/Å). In general, the B – H_t bonds in arachnoboranes (BSO: 0.834–0.999, k^a: 3.134–3.937 mdyn/Å) are stronger than the B – H_t bonds in closoboranes (BSO: 0.848–0.919, k^a: 3.201–3.541mdyn/Å) and weaker than the B – H_t bonds in nidoboranes (BSO: 0.759–1.026, itk^a: 2.781–4.074 mdyn/Å).

2.4. Thermal Decompositions, Intermediates, and Their Revesibility

Thermal decomposition of BH_4^- (2). The weakest B–H_t bond is found in BH_4^- (**2**) (BSO = 0.759, k^a = 2.781 mdyn/Å). Although the B–H_t bond in BH_4^- (**2**) is the weakest B–H_t bond among the

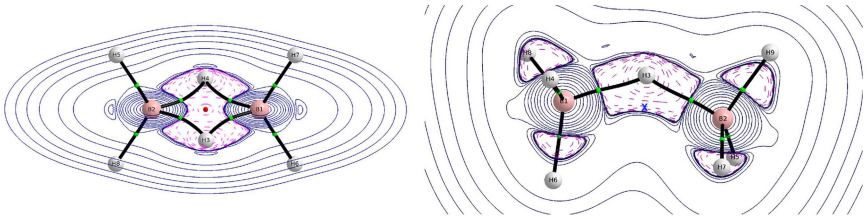

(a) B_2H_6 (**3**) (b) $B_2H_7^-$ (**4**)

Figure 5. The Laplacian contour plot of B_2H_6 (**3**) and $B_2H_7^-$ (**4**) in the B1H3B2H4 plane for B_2H_6 (**3**) and in the B2H3B2 plane for $B_2H_7^-$ (**4**). Continuous black solid lines correspond to the bond paths, green points refer to the bond critical points (BCPs), and the red point corresponds to a ring critical point (RCP).The dashed (pink) contours denote regions of charge concentration where $\nabla^2_{\rho(r)} < 0$ and the solid (blue) contours denote regions of charge depletion where $\nabla^2_{\rho(r)} < 0$. Blue cross corresponds to the point where the electron density ρ_c and energy densities H_c of $B_2H_7^-$ (**4**) were collected.

studied 21 boron-hydrogen compounds, BH_4^- (**2**) shows high thermal stability and sluggish kinetics.[35,141] The thermal decomposition of metal borohydrides occur at high temperature. The thermal decomposition of $LiBH_4$[142–145] and $Mg(BH_4)_2$[49,146,147] take place at 380 and 320 °C, respectively.

During the thermal decomposition, BH_4^- (**2**) releases hydrogen and forms many possible intermediates (see Figure 1). The formation of intermediates, such as $B_2H_7^-$ (**4**) and $B_3H_8^-$ (**5**), facilitate the reverse reactions,[47,54,59,62] due to their weak B–B–B and B–H_b–B bonds ($B_3H_8^-$ (**5**): BSO(B–B–B) = 0.415, k^a(B–B–B) = 0.824 mdyn/Å; BSO(B–H_b–B) = 0.188, k^a(B–H_b–B) = 0.477 mdyn/Å and $B_2H_7^-$ (**4**): BSO(B–B) = 0.265, k^a(B–B) = 0.296 mdyn/Å; BSO (B–H_b–B) = 0.058, k^a(B–H_b–B) = 0.109 mdyn/Å). The intermediates which facilitate the reverse reactions, such as $B_2H_7^-$ (**4**) and $B_3H_8^-$ (**5**) also show low thermodynamic stability[61,62] with ΔH_f^o −24.85 and −27.42 kcal/mol, respectively, as shown in Figure 3.

On the other hand, the formation of intermediate such as $B_{12}H_{12}^{2-}$ (**21**) hampers the reversibility of the hydrogenation/dehydrogenation reactions,[53–57] as it has strong B–B–B and B–H_t bonds (BSO(B–B–B) = 0.465, k^a(B–B–B) = 1.067 mdyn/Å; BSO(B–H_t) = 0.919, k^a(B–H_t) = 3.541 mdyn/Å). $B_{12}H_{12}^{2-}$ (**21**) also shows very high thermodynamic stability with ΔH_f^o: −102.43 kcal/mol (ΔH_f^o of BH_4^- (**2**) is −15.52 kcal/mol); the highest thermodynamics stability among the 21 studied compounds. McKee and Warneke noted that the high thermodynamics stability of $B_{12}H_{12}^{2-}$ (**21**) is attributed to both steric protection and electron donation provided by the counter ions.[63,148]

Selected Intermediates

B_2H_6 (3). Diborane, B_2H_6 (**3**), is the simplest stable boron-hydrogen compounds at ambient condition.[149] It has a ring-type molecular structure of two B and two-bridging hydrogen atoms. The bridging hydrogen bond is constructed by an electron deficient three center-two electron (3c–2e) B–H_b–B bond. The formation of diborane is observed during the thermal decomposition of *e.g.* $LiBH_4$,[47,48] $Mg(BH_4)_2$,[150] and $Mn(BH_4)_2$.[151] Although diborane has weak B–H_b–B bonds (k^a (B–H_b–B) = 0.904 mdyn/Å, BSO = 0.312), the formation of diborane hinder the reversibility of the dehydrogenation reaction due to the loss of boron (B_2H_6 (**3**) is a volatile gas).[152,153]

B_2H_6 (**3**) has both B–H_b–B and B–H_t bonds. The former bonds (k^a (B–H_b–B) = 0.904 mdyn/Å, BSO = 0.312) are weaker than the later bonds (k^a (B–H_t) = 3.903 mdyn/Å, BSO = 0.992). This is in line with the work of Popelier and co-workers, who found that the interaction energy of B–H_t (92.02 kcal/mol) is significantly larger than the interaction energy of B–H_b–B (53.06 kcal/mol).[154,155]

The bridging hydrogen bond, B–H_b–B, in B_2H_6 (**3**) has strongly inwardly bent (concave) bond paths as shown in Figure 5. The concave shape of the bond paths of B_2H_6 (**3**) is a result of the charge transfer donation from the B–B bond to the low-lying 2*s* orbital of H_b atom, while the back donation from H_b is less favorable as all low-lying molecular orbitals of B–B are occupied.[156]

$B_2H_7^-$ (4). The formation of $B_2H_7^-$ (**4**) has been observed during the thermal decomposition of $Mg(BH_4)_2$.[58–60] The formation of $B_2H_7^-$ (**4**) facilitates the reversibility of the reverse reaction due its weak B–B and B–H_b–B bonds. The B–B bond in $B_2H_7^-$ (**4**) is the weakest B–B–B bonds among the studied 21 boron-hydrogen compounds. The B–B bond in $B_2H_7^-$ (**4**) is the lowest covalent character among the studied 21 boron-hydrogen compounds (ρ_c: 0.651 *e*/Å^3 and H_c/ρ_c: −0.436 *h*/Å^3). $B_2H_7^-$ (**4**) also has low thermodynamic stability (ΔH_f^o: −24.85 kcal/mol).

It is also worth to mention that we do not observe bond path and bond critical points between B–B in B_2H_6 (**3**) and $B_2H_7^-$ (**4**) (BB lengths are 1.761 and 2.383 Å, respectively), as shown in Figure 5. However, several authors have argued that the absence of a bond path and bond critical point should not be viewed as evidence against the absence of the bonds, but rather missing one piece of evidence for chemical bonds.[157,158] Based on that argument, we collected the electron densities ρ_c and energy densities H_c of B_2H_6 (**3**) and $B_2H_7^-$ (**4**) on the middle point between two boron atoms (Table 3).

$B_3H_8^-$ (5). The formation of $B_3H_8^-$ (**5**) has been observed as an intermediate during the decomposition of *e.g.* $Mg(BH_4)_2$ and $Y(BH_4)_3$.[54,59,62] The formation of $B_3H_8^-$ (**5**) facilitates the

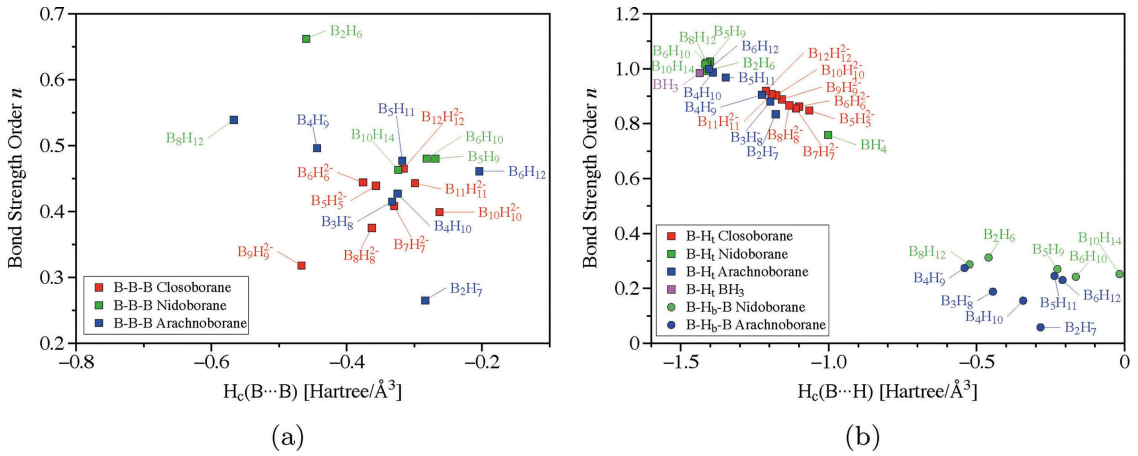

Figure 6. Plot of the bond strength order as a function of the total energy density H_c at B–B–B and B–H_b–B ring critical points (RCPs) and B–H_t bond critical points (BCPs) for (a) B–B–B and (b) B–H_b–B and B–H_t bonds in 21 boron-hydrogen species, calculated at B3LYP-D2/cc-pVTZ level of theory.

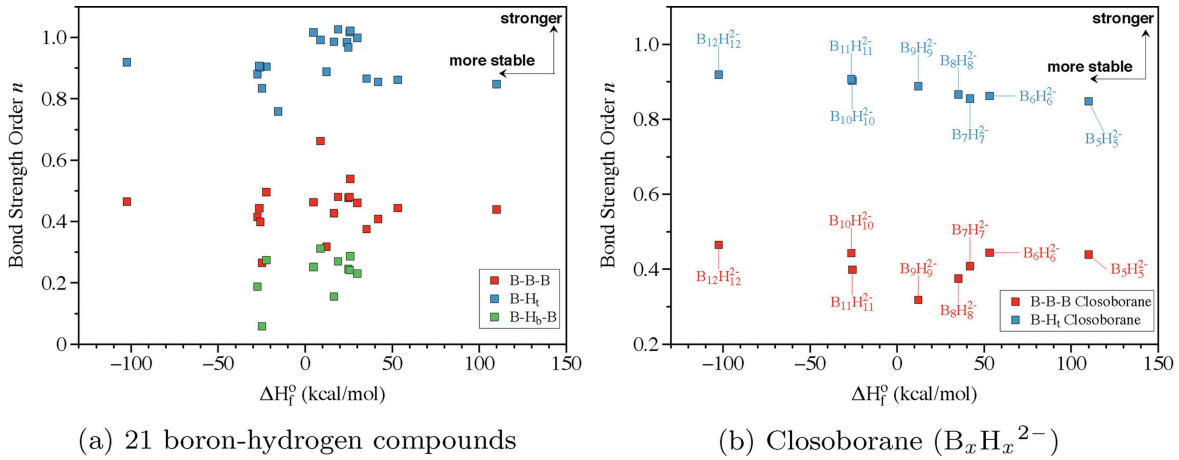

Figure 7. Plot of the bond strength order of (a) 21 boron-hydrogen compounds and (b) closoboranes $B_xH_x^{2-}$ as a functions of heats of formation.

reversibility of the dehydrogenation reaction because of the weak B–H_b–B bonds. $B_3H_8^-$ (**5**) has both B–H_b–B and B–H_t bonds. The former bonds (k^a (B–H_b–B) = 0.477 mdyn/Å, BSO = 0.188) are weaker than the later bonds (k^a (B–H_t) = 3.351 mdyn/Å, BSO = 0.880). The B–H_b–B bond has lower covalent character (H_c = -0.445 e/Å^3, H_c/ρ_c = −0.585 h/e) than those of the B–H_t bond (H_c = -1.197 e/Å^3, H_c/ρ_c = -1.049 h/e) (see Figure 6). The B–H_b–B bond in $B_3H_8^-$ (**5**) is stronger than the B–H_b–B bond in B_2H_6 (**3**), while the B–H_t bond in $B_3H_8^-$ (**5**) is weaker than the B–H_t bond in B_2H_6 (**3**).

$B_{12}H_{12}^{2-}$ $B_{12}H_{12}^{2-}$ (21). $B_{12}H_{12}^{2-}$ is the most stable boron-hydrogen compounds investigated in this work. The formation of $B_{12}H_{12}^{2-}$ has been observed as an intermediate during the decomposition of *e.g.* $LiBH_4$ and $Mg(BH_4)_2$.[51,52,62] The formation of $B_{12}H_{12}^{2-}$ hinders the reversibility of hydrogenation/dehydrogenation reactions due to their strong B–B–B and B–H_t, and their thermodynamic stability (see detailed explanation in paragraph Thermal decomposition of BH_4^-). The B–H_t bonds in $B_{12}H_{12}^{2-}$ (**21**) is the strongest among closoboranes ($B_xH_x^{2-}$) investigated in this work.

2.5. The Local Mode Analysis as a Predictive Tool

As shown in this work, thermodynamic data paired with the intrinsic bond strength provide an effective tool to explain and to predict why and under which circumstances intermediate boron-hydride compounds facilitate or impede the reversibility of the hydrogenation/dehydrogenation reactions. The thermal decomposition of borohydrides and their reverse reactions involve bond breaking and bond forming of B–B–B, B–H_b–B, and B–H_t bonds; therefore intermediates, which are characterized by strong B–B–B, B–H_b–B, and B–H_t bonds and high thermal stability hamper the reversibility of the reactions, while intermediates, which are characterized by weak B–B–B, B–H_b–B, and B–H_t bonds and low thermal stability, facilitate them.

There is no correlation between the heats of formation and the BB or BH bonds strength order for the 21 boron-hydrogen compounds investigated in this work (see Figure 7(a)) reflecting that the heat of formation is a cumulative property, while the intrinsic bond strength concern just an individual part of the molecule. For example, the heats of formation of $B_5H_5^{2-}$ and

$B_{12}H_{12}^{2-}$ are +109.91 and −102.43 kcal/mol, respectively; while the BSO of B–B–B and B–H_t in $B_5H_5^{2-}$ and $B_{12}H_{12}^{2-}$ are slightly different ($B_5H_5^{2-}$: BSO(B–B–B) = 0.439 and BSO(B–H_t) = 0.848; $B_{12}H_{12}^{2-}$: BSO(B–B–B) = 0.465 and BSO(B–H_t) = 0.919) as shown in Figure 7(b)). Therefore, heats of formation and bond strength order are complementary, and as such they form an efficient tool to characterize intermediates and their role for the reversibility of hydrogenation/dehydrogenation reactions.

The intrinsic strength of the B–B–B, B–H_b–B, and B–H_t bonds are attributed to a combination of multiple factors, with the covalent character playing a key role. We observed that strong bonds possess a high electron density between a bond, while weak bonds have lower electron density. The B–H_t bond is significantly stronger than the three center-two electron (3c–2e) B–H_b–B bond. The (nido- and arachnoboranes) intermediates such as $B_4H_9^-$ and B_5H_9, which possess weak B–B–B, B–H_b–B, and B–H_t bonds, and low thermodynamic stability, are good candidates to be isolated as new intermediates for reversible hydrogenation/dehydrogenation reactions.

3. Concluding Remarks

We present in this work for the first time a quantitative and detailed analysis of the intrinsic multicenter B–B–B and B–H_b–B, and B–H_t bond strengths complemented by calculated heats of formation for 21 boron-hydrogen compounds ranging from BH_3 to $B_{12}H_{12}^{2-}$. The chosen B3LYP-D2 model chemistry provides reasonable geometries compared to experimental data and G4 predicts heats of formation close to the experimental values. For n smaller than 6 (where n is the number of boron atoms), G4 provides enthalpies with a maximum deviation of about 3 kcal/mol, while for n larger than 6, deviations may reach up to 10 kcal/mol.

Hydrogenation and dehydrogenation reactions involve breaking and forming of B–B–B, B–H_b–B, and B–H_t bonds. The use of the thermodynamic data and the intrinsic bonds strength forms a new powerful tool to characterize new (potential) intermediates and their role for the reversibility of hydrogenation/dehydrogenation reactions. Based on our study, we proposed that intermediates, which are characterized by weak B–B–B, B–H_b–B, and B–H_t bonds and low thermodynamic stability, facilitate the reversibility of hydrogenation/dehydrogenation reactions; while intermediates, which are characterized by strong B–B–B, B–H_b–B, and B–H_t covalent bonds and high thermodynamic stability, impede the reversibility. This could be confirmed for all experimentally observed intermediates, proving the correctness of our proposal.

The intrinsic strength of the B–B–B, B–H_b–B, and B–H_t bonds are determined by a combination of multiple factors, with the covalent character playing a key role. The stronger bonds have a higher percentage of covalent characters, while the weak bonds have less. The B–H_t bond is significantly stronger than the three center-two electron (3c–2e) B–H_b–B bond. Intermediate (nido- and arachnoboranes) species, such as $B_4H_9^-$ and B_5H_9, possessing weak three center-two electron (3c–2e) B–H_b–B bonds and low thermodynamic stability are good candidates to be isolated in the experiments for reversible hydrogenation/dehydrogenation reactions, to be used as hydrogen storage materials.

The intrinsic bond strength may be changed by the influence of counter ions and crystal packing effects. This will be studied in more detail in future work. Our analysis revealed the existence of a recently proposed B–B–B–B 4-center-2-electron bond,[159] which will also be the subject of a future investigation.

Acknowledgment

This work was supported by the National Science Foundation (Grant CHE 1464906) and the Swiss National Science Foundation (project 200021-169033). The authors thank Southern Methodist University and the University of Geneva for providing excellence computational resources. DS thanks to Dr. Velmurugan Gunasekaran, Dr. Alan Humason, Dr. Vytor Pinheiro Oliveira, and Niraj Verma for fruitful discussions.

Conflict of Interest

The authors declare no conflict of interest.

Keywords: boron-hydrogen compounds · dehydrogenation · hydrogenation · intrinsic bond strength · local mode force constants

[1] D. Hnyk, M. McKee, *Boron: The Fifth Element*, Springer, Switzerland, **2015**.
[2] W. N. Lipscomb, *Boronhydrides*, W. A. Benjamin, New York, **2013**.
[3] M. Li, J. S. Fossey, T. D. James, (Eds.) *Boron: Sensing, Synthesis and Supramolecular Self-Assembly*, RSC, Cambridge, UK, **2016**.
[4] M. Davidson, A. K. Hughes, T. B. Marder, K. Wade, *Contemporary Boron Chemistry*, RSC, Cambridge, **2000**.
[5] M. Paskevicius, L. H. Jepsen, P. Schouwink, R. Černý, D. B. Ravnsbæk, Y. Filinchuk, M. Dornheim, F. Besenbacher, T. R. Jensen, *Chem. Soc. Rev.* **2017**, *46*, 1565–1634.
[6] B. R. Hansen, M. Paskevicius, H.-W. Li, E. Akiba, T. R. Jensen, *Coord. Chem. Rev.* **2016**, *323*, 60–70.
[7] J. Puszkiel, S. Garroni, C. Milanese, F. Gennari, T. Klassen, M. Dornheim, C. Pistidda, *Inorganics* **2017**, *5*, 74–1–74–24.
[8] Z. Wang, J. Parrondo, C. He, S. Sankarasubramanian, V. Ramani, *Nat. Energy* **2019**, *4*, 281–289.
[9] L. Duchêne, R.-S. Kühnel, D. Rentsch, A. Remhof, H. Hagemann, C. Battaglia, *Chem. Commun.* **2017**, *53*, 4195–4198.
[10] W. S. Tang, M. Matsuo, H. Wu, V. Stavila, W. Zhou, A. A. Talin, A. V. Soloninin, R. V. Skoryunov, O. A. Babanova, A. V. Skripov, A. Unemoto, S.-I. Orimo, T. J. Udovic, *Adv. Energy Mater.* **2016**, *6*, 1502237.
[11] Y. Sadikin, M. Brighi, P. Schouwink, R. Černý, *Adv. Energy Mater.* **2015**, *5*, 1501016.
[12] I. B. Sivaev, V. I. Bregadze, N. T. Kuznetsov, *Russ. Chem. Bull.* **2002**, *51*, 1362–1374.
[13] M. F. Hawthorne, A. Maderna, *Chem. Rev.* **1999**, *99*, 3421–3434.
[14] A. H. Soloway, W. Tjarks, B. A. Barnum, F.-G. Rong, R. F. Barth, I. M. Codogni, J. G. Wilson, *Chem. Rev.* **1998**, *98*, 1515–1562.
[15] M. F. Hawthorne, *Mol. Med. Today* **1998**, *4*, 174–181.
[16] W. Zou, X. Zhang, H. Dai, H. Yan, D. Cremer, E. Kraka, *J. Org. Chem.* **2018**, *865*, 114–127.
[17] X. Zhang, H. Dai, H. Yan, W. Zou, D. Cremer, *J. Am. Chem. Soc.* **2016**, *138*, 4334–4337.
[18] P. K. Bhattacharyya, *New J. Chem.* **2017**, *41*, 1293–1302.

[19] B. Saha, P. K. Bhattacharyya, *New J. Chem.* **2017**, *41*, 5040–5054.
[20] J. Fanfrlík, A. Pecina, J. Řezáč, R. Sedlak, D. Hnyk, M. Lepšík, P. Hobza, *Phys. Chem. Chem. Phys.* **2017**, *19*, 18194–18200.
[21] P. Ravinder, V. Subramanian, *J. Phys. Chem. A* **2010**, *114*, 5565–5572.
[22] H. Li, D. Min, S. G. Shore, W. N. Lipscomb, W. Yang, *Inorg. Chem.* **2007**, *46*, 3956–3959.
[23] Z. Konkoli, D. Cremer, *Int. J. Quantum Chem.* **1998**, *67*, 1.
[24] Z. Konkoli, J. A. Larsson, D. Cremer, *Int. J. Quantum Chem.* **1998**, *67*, 41.
[25] W. Zou, R. Kalescky, E. Kraka, D. Cremer, *J. Chem. Phys.* **2012**, *137*, 084114.
[26] E. Kraka, J. A. Larsson, D. Cremer, in *Computational Spectroscopy*, Wiley-VCH Verlag GmbH & Co. KGaA, **2010**, (pages 105–149).
[27] R. Kalescky, W. Zou, E. Kraka, D. Cremer, *Chem. Phys. Lett.* **2012**, *554*, 243–247.
[28] M. Freindorf, E. Kraka, D. Cremer, *Int. J. Quantum Chem.* **2012**, *112*, 3174–3187.
[29] A. V. Skripov, R. V. Skoryunov, A. V. Soloninin, O. A. Babanova, W. S. Tang, V. Stavila, T. J. Udovic, *J. Phys. Chem. C* **2015**, *119*, 26912–26918.
[30] H. Wu, W. S. Tang, W. Zhou, J. D. Tarver, V. Stavila, C. M. Brown, T. J. Udovic, *J. Solid State Chem.* **2016**, *243*, 162–167.
[31] M. Sharma, D. Sethio, V. D'Anna, H. Hagemann, *Int. J. Hydrogen Energy* **2015**, *40*, 12721–12726.
[32] L. Duchêne, R.-S. Kühnel, E. Stilp, E. C. Reyes, A. Remhof, H. Hagemann, C. Battaglia, *Energy Environ. Sci.* **2017**, *10*, 2609–2615.
[33] L. Schlapbach, A. Züttel, *Nature* **2001**, *414*, 353–358.
[34] M. Sharma, D. Sethio, V. D'Anna, J. C. Fallas, P. Schouwink, R. Černý, H. Hagemann, *J. Phys. Chem. C* **2014**, *119*, 29–32.
[35] A. Züttel, A. Borgschulte, S.-I. Orimo, *Scr. Mater.* **2007**, *56*, 823–828.
[36] S.-I. Orimo, Y. Nakamori, J. R. Eliseo, A. Züttel, C. M. Jensen, *Chem. Rev.* **2007**, *107*, 4111–4132.
[37] Y. Liu, S. Giri, J. Zhou, P. Jena, *J. Phys. Chem. C* **2014**, *118*, 28456–28461.
[38] M. Fichtner, K. Chlopek, M. Longhini, H. Hagemann, *J. Phys. Chem. C* **2008**, *112*, 11575–11579.
[39] J.-H. Kim, J.-H. Shim, Y. W. Cho, *J. Power Sources* **2008**, *181*, 140–143.
[40] Y. Nakamori, K. Miwa, A. Ninomiya, H. Li, N. Ohba, S.-I. Towata, A. Züttel, S.-I. Orimo, *Phys. Rev. B* **2006**, *74*.
[41] X. X. Hou, M. Sulic, J. P. Ortmann, M. Cai, A. Chakraborty, *Int. J. Hydrogen Energy* **2016**, *41*, 4026–4038.
[42] Z. Lodziana, P. Błoński, Y. Yan, D. Rentsch, A. Remhof, *J. Phys. Chem. C* **2014**, *118*, 6594–6603.
[43] M. Paskevicius, M. P. Pitt, C. J. Webb, D. A. Sheppard, U. Filsø, E. M. Gray, C. E. Buckley, *J. Phys. Chem. C* **2012**, *116*, 15231–15240.
[44] E. Callini, Z. Ö. K. Atakli, B. C. Hauback, S.-i. Orimo, C. Jensen, M. Dornheim, D. Grant, Y. W. Cho, P. Chen, B. Hjörvarsson, P. de Jongh, C. Weidenthaler, M. Baricco, M. Paskevicius, T. R. Jensen, M. E. Bowden, T. S. Autrey, A. Züttel, *Appl. Phys. A* **2016**, *122*, 353.
[45] L. H. Jepsen, M. B. Ley, Y.-S. Lee, Y. W. Cho, M. Dornheim, J. O. Jensen, Y. Filinchuk, J. E. Jørgensen, F. Besenbacher, T. R. Jensen, *Mater. Today* **2014**, *17*, 129–135.
[46] M. B. Ley, L. H. Jepsen, Y.-S. Lee, Y. W. Cho, J. M. B. von Colbe, M. Dornheim, M. Rokni, J. O. Jensen, M. Sloth, Y. Filinchuk, J. E. Jørgensen, F. Besenbacher, T. R. Jensen, *Mater. Today* **2014**, *17*, 122–128.
[47] B. Richter, D. Ravnsbæk, M. Sharma, A. S. Stratmann, H. Hagemann, T. R. R. Jensen, *Phys. Chem. Chem. Phys.* **2017**.
[48] O. Friedrichs, A. Remhof, S.-J. Hwang, A. Züttel, *Chem. Mater.* **2010**, *22*, 3265–3268.
[49] R. J. Newhouse, V. Stavila, S.-J. Hwang, L. E. Klebanoff, J. Z. Zhang, *J. Phys. Chem. C* **2010**, *114*, 5224–5232.
[50] N. Ohba, K. Miwa, M. Aoki, T. Noritake, S.-I. Towata, Y. Nakamori, S.-I. Orimo, A. Züttel, *Phys. Rev. B* **2006**, *74*, 075110, 00000.
[51] S.-J. Hwang, R. C. Bowman, J. W. Reiter, J. W. Rijssenbeek, G. L. Soloveichik, J.-C. Zhao, H. Kabbour, C. C. Ahn, *J. Phys. Chem. C* **2008**, *112*, 3164–3169.
[52] S.-I. Orimo, Y. Nakamori, N. Ohba, K. Miwa, M. Aoki, S.-I. Towata, A. Züttel, *Appl. Phys. Lett.* **2006**, *89*, 021920.
[53] T. Peymann, C. B. Knobler, S. I. Khan, M. F. Hawthorne, *Angew. Chem. Int. Ed.* **2001**, *40*, 1664–1667; *Angew. Chem.* **2001**, *113*, 1713–1715.
[54] Y. Yan, A. Remhof, D. Rentsch, Y.-S. Lee, Y. W. Cho, A. Züttel, *Chem. Commun.* **2013**, *49*, 5234.
[55] A. Remhof, Y. Yan, D. Rentsch, A. Borgschulte, C. M. Jensen, A. Züttel, *J. Mater. Chem. A* **2014**, *2*, 7244–7249.
[56] Y. Yan, A. Remhof, D. Rentsch, A. Züttel, *Chem. Commun.* **2015**, *51*, 700–702.
[57] S. R. H. Jensen, M. Paskevicius, B. R. S. Hansen, A. S. Jakobsen, K. T. Møller, J. L. White, M. D. Allendorf, V. Stavila, J. Skibsted, T. R. Jensen, *Phys. Chem. Chem. Phys.* **2018**, *20*, 16266–16275.
[58] K.-B. Kim, J.-H. Shim, Y. W. Cho, K. H. Oh, *Chem. Commun.* **2011**, *47*, 9831–9833.
[59] M. Chong, A. Karkamkar, T. Autrey, S.-I. Orimo, S. Jalisatgi, C. M. Jensen, *Chem. Commun.* **2011**, *47*, 1330–1332, 00033.
[60] J. Yang, X. Zhang, J. Zheng, P. Song, X. Li, *Scr. Mater.* **2011**, *64*, 225–228.
[61] J. K. Olson, A. I. Boldyrev, *Comput. Theor. Chem.* **2011**, *967*, 1–4.
[62] M. Chong, M. Matsuo, S.-I. Orimo, T. Autrey, C. M. Jensen, *Inorg. Chem.* **2015**, *54*, 4120–4125.
[63] M. L. McKee, *Inorg. Chem.* **1999**, *38*, 321–330.
[64] M. L. McKee, Z.-X. Wang, P. von Ragué Schleyer, *J. Am. Chem. Soc.* **2000**, *122*, 4781–4793.
[65] M. Sharma, D. Sethio, L. M. L. Daku, H. Hagemann, *J. Phys. Chem. A* **2019**, *123*, 1807–1813.
[66] H. S. Rzepa, S. Arkhipenko, E. Wan, M. T. Sabatini, V. Karaluka, A. Whiting, T. D. Sheppard, *J. Org. Chem.* **2018**, *83*, 8020–8025.
[67] M. Hofmann, P. von Ragué Schleyer, *Inorg. Chem.* **1999**, *38*, 652–660.
[68] M. Hofmann, P. von Ragué Schleyer, *Inorg. Chem.* **1998**, *37*, 5557–5565.
[69] M. Buhl, J. Gauss, M. Hofmann, P. v. R. Schleyer, *J. Am. Chem. Soc.* **1993**, *115*, 12385–12390.
[70] M. Buehl, P. v. R. Schleyer, *J. Am. Chem. Soc.* **1992**, *114*, 477–491.
[71] H. Braunschweig, T. Dellermann, R. D. Dewhurst, B. Hupp, T. Kramer, J. D. Mattock, J. Mies, A. K. Phukan, A. Steffen, A. Vargas, *J. Am. Chem. Soc.* **2017**, *139*, 4887–4893.
[72] K. K. Bania, A. K. Guha, P. K. Bhattacharyya, *J. Chem. Phys.* **2016**, *145*, 184112.
[73] D. Setiawan, E. Kraka, D. Cremer, *J. Phys. Chem. A* **2015**, *119*, 9541–9556.
[74] D. Cremer, J. A. Larsson, E. Kraka, in C. Parkanyi, (Ed.) *Theoretical and Computational Chemistry*, Elsevier, Amsterdam, **1998**, (pages 259–327).
[75] R. Kalescky, E. Kraka, D. Cremer, *J. Phys. Chem. A* **2014**, *118*, 223–237.
[76] D. Cremer, E. Kraka, *Curr. Org. Chem.* **2010**, *14*, 1524–1560.
[77] E. Kraka, D. Setiawan, D. Cremer, *J. Comb. Chem.* **2016**, *37*, 130–142.
[78] W. Zou, R. Kalescky, E. Kraka, D. Cremer, *J. Mol. Model.* **2012**, *19*, 2865–2877.
[79] A. Humason, W. Zou, D. Cremer, *J. Phys. Chem. A* **2015**, *119*, 1666–1682.
[80] R. Kalescky, E. Kraka, D. Cremer, *J. Phys. Chem. A* **2013**, *117*, 8981–8995.
[81] D. Setiawan, D. Sethio, D. Cremer, E. Kraka, *Phys. Chem. Chem. Phys.* **2018**, *20*, 23913–23927.
[82] R. Kalescky, E. Kraka, D. Cremer, *Inorg. Chem.* **2014**, *53*, 478–495.
[83] E. Kraka, D. Cremer, *ChemPhysChem* **2009**, *10*, 686–698.
[84] R. Kalescky, E. Kraka, D. Cremer, *Int. J. Quantum Chem.* **2014**, *114*, 1060–1072.
[85] R. Kalescky, W. Zou, E. Kraka, D. Cremer, *J. Phys. Chem. A* **2014**, *118*, 1948–1963.
[86] J. Oomens, E. Kraka, M. K. Nguyen, T. H. Morton, *J. Phys. Chem. A* **2008**, *112*, 10774–10783.
[87] M. Freindorf, E. Kraka, D. Cremer, *Int. J. Quantum Chem.* **2012**, *112*, 3174–3187.
[88] R. Kalescky, W. Zou, E. Kraka, D. Cremer, *Chem. Phys. Lett.* **2012**, *554*, 243–247.
[89] R. Kalescky, E. Kraka, D. Cremer, *Mol. Phys.* **2013**, *111*, 1497–1510.
[90] E. Kraka, M. Freindorf, D. Cremer, *Chirality* **2013**, *25*, 185–196.
[91] V. Oliveira, E. Kraka, D. Cremer, *Phys. Chem. Chem. Phys.* **2016**, *18*, 33031–33046.
[92] V. Oliveira, E. Kraka, *J. Phys. Chem. A* **2017**, *121*, 9544–9556.
[93] V. Oliveira, D. Cremer, *Chem. Phys. Lett.* **2017**, *681*, 56–63.
[94] D. Setiawan, E. Kraka, D. Cremer, *J. Phys. Chem. A* **2014**, *119*, 1642–1656.
[95] D. Setiawan, E. Kraka, D. Cremer, *Chem. Phys. Lett.* **2014**, *614*, 136–142.
[96] D. Setiawan, D. Cremer, *Chem. Phys. Lett.* **2016**, *662*, 182–187.
[97] D. Sethio, V. Oliveira, E. Kraka, *Molecules* **2018**, *23*, 2763.
[98] H. Hagemann, M. Sharma, D. Sethio, L. M. Lawson Daku, *Helv. Chim. Acta* **2018**, *101*, e1700239.
[99] D. Sethio, *Critical evaluation of the effect of an harmonicity and dispersion interactions using density functional theory on structural and spectroscopic properties of selected inorganic compounds*, phdthesis, University of Geneva, **2017**, URL https://archive-ouverte.unige.ch/unige:96319.
[100] D. Sethio, L. M. Lawson Daku, H. Hagemann, *Int. J. Hydrogen Energy* **2017**, *42*, 22496–22501.

[101] D. Sethio, L. M. Lawson Daku, H. Hagemann, *Int. J. Hydrogen Energy* **2016**, *41*, 6814–6824.
[102] A. D. Becke, *J. Chem. Phys.* **1993**, *98*, 5648–5652.
[103] S. Grimme, *J. Comput. Chem.* **2006**, *27*, 1787–1799.
[104] T. H. Dunning, *J. Chem. Phys.* **1989**, *90*, 1007–1023.
[105] R. A. Kendall, T. H. Dunning, R. J. Harrison, *J. Chem. Phys.* **1992**, *96*, 6796–6806.
[106] L. A. Curtiss, P. C. Redfern, K. Raghavachari, *J. Chem. Phys.* **2007**, *126*, 084108.
[107] M. T. Nguyen, M. H. Matus, D. A. Dixon, *Inorg. Chem.* **2007**, *46*, 7561–7570.
[108] R. Maillard, D. Sethio, H. Hagemann, L. M. Lawson Daku, *ACS omega* **2019**, in press.
[109] C.-L. Yu, S. H. Bauer, *J. Phys. Chem. Ref. Data* **1998**, *27*, 807–835.
[110] E. B. Wilson, J. C. Decius, P. C. Cross, *Molecular Vibrations. The Theory of Infrared and Raman Vibrational Spectra*, McGraw-Hill: New York, **1955**.
[111] K. Wiberg, *Tetrahedron* **1968**, *24*, 1083–1096.
[112] I. Mayer, *J. Comput. Chem.* **2007**, *28*, 204.
[113] M. J. Frisch, G. W. Trucks, H. B. Schlegel, G. E. Scuseria, M. A. Robb, J. R. Cheeseman, G. Scalmani, V. Barone, B. Mennucci, G. A. Petersson, H. Nakatsuji, M. Caricato, X. Li, H. P. Hratchian, A. F. Izmaylov, J. Bloino, G. Zheng, J. L. Sonnenberg, M. Hada, M. Ehara, K. Toyota, R. Fukuda, J. Hasegawa, M. Ishida, T. Nakajima, Y. Honda, O. Kitao, H. Nakai, T. Vreven, J. A. Montgomery, Jr., J. E. Peralta, F. Ogliaro, M. Bearpark, J. J. Heyd, E. Brothers, K. N. Kudin, V. N. Staroverov, Kobayashi, J. Normand, K. Raghavachari, A. Rendell, J. C. Burant, S. Iyengar, J. Tomasi, M. Cossi, N. Rega, J. M. Millam, M. Klene, J. E. Knox, J. B. Cross, V. Bakken, C. Adamo, J. Jaramillo, R. Gomperts, R. E. Stratmann, O. Yazyev, A. J. Austin, R. Cammi, C. Pomelli, J. W. Ochterski, R. L. Martin, K. Morokuma, V. G. Zakrzewski, G. A. Voth, P. Salvador, J. J. Dannenberg, S. Dapprich, A. D. Daniels, O. Farkas, J. B. Foresman, J. V. Ortiz, J. Cioslowski, D. J. Fox, Gaussian 09 Revision D.01, gaussian Inc. Wallingford CT 2009.
[114] J. Gräfenstein, D. Cremer, *J. Chem. Phys.* **2007**, *127*, 164113.
[115] E. Kraka, M. Filatov, W. Zou, J. Grafenstein, D. Izotov, J. Gauss, Y. He, A. Wu, V. Polo, L. Olsson, Z. Konkoli, Z. He, D. Cremer, COLOGNE2017, **2017**, Southern Methodist University, Dallas, TX.
[116] R. Bader, *Chem. Rev.* **1991**, *91*, 893.
[117] R. Bader, *Atoms in Molecules: A Quantum Theory*, Oxford University Press, **1994**.
[118] R. Bader, *Chem. Rev.* **1998**, *1*, 64.
[119] T. Keith, TK Gristmill Software, **2011**, overland Park KS, USA; see http// aim.tkgristmill.com.
[120] D. Cremer, E. Kraka, *Angew. Chem. Int. Ed. Engl.* **1984**, *23*, 627.
[121] D. Cremer, E. Kraka, *Croat. Chem. Acta* **1984**, *57*, 1259.
[122] E. Kraka, D. Cremer, in Z. Maksic, (Ed.) *Theoretical Models of Chemical Bonding. The Concept of the Chemical Bond, Vol 2*, Springer Verlag, Heidelberg, Germany, **1990**, (page 453).
[123] K. Kawaguchi, *J. Chem. Phys.* **1992**, *96*, 3411–3415.
[124] G. Renaudin, S. Gomes, H. Hagemann, L. Keller, K. Yvon, *J. Alloys Compd.* **2004**, *375*, 98–106.
[125] L. S. Bartell, B. L. Carroll, *J. Chem. Phys.* **1965**, *42*, 1135–1139.
[126] S. I. Khan, M. Y. Chiang, R. Bau, T. F. Koetzle, S. G. Shore, S. H. Lawrence, *J. Chem. Soc. Dalton Trans.* **1986**, *0*, 1753–1757.
[127] Z. Huang, G. King, X. Chen, J. Hoy, T. Yisgedu, H. K. Lingam, S. G. Shore, P. M. Woodward, J.-C. Zhao, *Inorg. Chem.* **2010**, *49*, 8185–8187.
[128] C. J. Dain, A. J. Downs, G. S. Laurenson, D. W. H. Rankin, *J. Chem. Soc. Dalton Trans.* **1981**, *0*, 472.
[129] D. Schwoch, A. B. Burg, R. A. Beaudet, *Inorg. Chem.* **1977**, *16*, 3219–3222.
[130] R. Greatrex, N. N. Greenwood, D. W. H. Rankin, H. E. Robertson, *Polyhedron* **1987**, *6*, 1849–1858.
[131] V. K. Kochnev, V. V. Avdeeva, L. V. Goeva, E. A. Malinina, N. T. Kuznetsov, *Russ. J. Inorg. Chem.* **2015**, *60*, 1110–1116.
[132] F. Schlüter, E. Bernhardt, *Inorg. Chem.* **2011**, *50*, 2580–2589.
[133] L. J. Guggenberger, *Inorg. Chem.* **1969**, *8*, 2771–2774.
[134] R. E. Enrione, F. P. Boer, W. N. Lipscomb, *Inorg. Chem.* **1964**, *3*, 1659–1666.
[135] K. Siegburg, W. Preetz, *Inorg. Chem.* **2000**, *39*, 3280–3282.
[136] K. Hofmann, B. Albert, *Z. Kristallogr.* **2005**, *220*.
[137] A. Tippe, W. C. Hamilton, *Inorg. Chem.* **1969**, *8*, 464–470.
[138] E. G. Kononova, L. A. Leites, S. S. Bukalov, I. V. Pisareva, I. T. Chizhevsky, J. D. Kennedy, J. Bould, *Eur. J. Inorg. Chem.* **2007**, *2007*, 4911–4918.
[139] M. Yousufuddin, J.-H. Her, W. Zhou, S. S. Jalisatgi, T. J. Udovic, *Inorg. Chim. Acta* **2009**, *362*, 3155–3158.
[140] S. R. Gunn, J. H. Kindsvater, *J. Chem. Phys.* **1966**, *70*, 1114–1119.
[141] J. Yang, A. Sudik, C. Wolverton, *J. Phys. Chem. C* **2007**, *111*, 19134–19140.
[142] A. Züttel, S. Rentsch, P. Fischer, P. Wenger, P. Sudan, P. Mauron, C. Emmenegger, *J. Alloys Compd.* **2003**, *356–357*, 515–520.
[143] J. Mao, Z. Guo, H. Liu, X. Yu, *J. Alloys Compd.* **2009**, *487*, 434–438.
[144] P. Mauron, F. Buchter, O. Friedrichs, A. Remhof, M. Bielmann, C. N. Zwicky, A. Zttel, *J. Phys. Chem. B* **2008**, *112*, 906–910.
[145] X. B. Yu, D. M. Grant, G. S. Walker, *J. Phys. Chem. C* **2009**, *113*, 17945–17949.
[146] K. Chłopek, C. Frommen, A. Léon, O. Zabara, M. Fichtner, *J. Mater. Chem.* **2007**, *17*, 3496.
[147] H.-W. Li, K. Kikuchi, Y. Nakamori, K. Miwa, S. Towata, S. Orimo, *Scr. Mater.* **2007**, *57*, 679–682.
[148] J. Warneke, G.-L. Hou, E. Aprà, C. Jenne, Z. Yang, Z. Qin, K. Kowalski, X.-B. Wang, S. S. Xantheas, *J. Am. Chem. Soc.* **2017**, *139*, 14749–14756.
[149] W. N. Limpscomb, *Boron hydrides*, New York: W. A. Benjamin, **1963**.
[150] C. Jensen, Fundamental study of high capacity reversible metal hydride, Technical report, Department of Energy, **2007**.
[151] J.-C. Zhao, M. Andrus, Light weight intermetallics for hydrogen storage, Technical report, Department of Energy, **2007**.
[152] M. Au, R. T. Walters, *Int. J. Hydrogen Energy* **2010**, *35*, 10311–10316.
[153] W. Cai, H. Wang, L. Jiao, Y. Wang, M. Zhu, *Int. J. Hydrogen Energy* **2013**, *38*, 3304–3312.
[154] P. L. A. Popelier, in *Applications of Topological Methods in Molecular Chemistry*, Springer International Publishing, **2016**, (pages 23–52).
[155] M. García-Revilla, E. Francisco, P. L. A. Popelier, A. M. Pendás, *ChemPhysChem* **2013**, *14*, 1211–1218.
[156] D. Cremer, E. Kraka, *J. Am. Chem. Soc.* **1985**, *107*, 3800–3810.
[157] J. R. Lane, J. Contreras-García, J.-P. Piquemal, B. J. Miller, H. G. Kjaergaard, *J. Chem. Theory Comput.* **2013**, *9*, 3263–3266.
[158] M. Mousavi, G. Frenking, *Organometallics* **2013**, *32*, 1743–1751.
[159] P. Melichar, D. Hnyk, J. Fanfrlík, *Phys. Chem. Chem. Phys.* **2018**, *20*, 4666–4675.

Manuscript received: April 11, 2019
Revised manuscript received: May 6, 2019
Accepted manuscript online: May 7, 2019
Version of record online: July 3, 2019